

ChemComm

Chemical Communications

Accepted Manuscript

This article can be cited before page numbers have been issued, to do this please use: S. M. Ghoreishian, M. Norouzi and J. Lauterbach, *Chem. Commun.*, 2025, DOI: 10.1039/D4CC06382A.



This is an Accepted Manuscript, which has been through the Royal Society of Chemistry peer review process and has been accepted for publication.

Accepted Manuscripts are published online shortly after acceptance, before technical editing, formatting and proof reading. Using this free service, authors can make their results available to the community, in citable form, before we publish the edited article. We will replace this Accepted Manuscript with the edited and formatted Advance Article as soon as it is available.

You can find more information about Accepted Manuscripts in the [Information for Authors](#).

Please note that technical editing may introduce minor changes to the text and/or graphics, which may alter content. The journal's standard [Terms & Conditions](#) and the [Ethical guidelines](#) still apply. In no event shall the Royal Society of Chemistry be held responsible for any errors or omissions in this Accepted Manuscript or any consequences arising from the use of any information it contains.

Recent progress in the decomposition of ammonia as potential hydrogen-carrier by green technologies

Seyed Majid Ghoreishian, Mohammad Norouzi, Jochen Lauterbach*

^a *Department of Chemical Engineering, University of South Carolina, Columbia, SC 29208, USA.*

^b *School of Cancer Sciences, University of Glasgow, Glasgow, UK.*

*Corresponding author

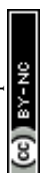
E-mail address: lauteraj@cec.sc.edu (J. Lauterbach)



Abstract

To meet the global carbon neutrality target set by the United Nations, finding alternative and cost-effective energy sources has become prominent while enhancing energy conversion methods' efficiency. The versatile applications of hydrogen (H_2) as an energy vector have been highly valued over the past decades due to its significantly lower greenhouse gas emissions compared to conventional fossil fuels. However, challenges related to H_2 generation and storage for portable applications have increasingly called attention to ammonia (NH_3) decomposition as an effective method of on-site hydrogen production due to its characteristic high hydrogen content, high energy density, and affordability. This review highlights recent developments in green decomposition techniques of ammonia, including catalytic membrane reactors, microchannel reactors, thermochemical processes, non-thermal plasma, solar-driven decomposition, and electrolysis, with a focus on the latest developments in new methods and materials (catalysts, electrodes, and sorbents) employed in these processes. Moreover, technical challenges and recommendations are discussed to assess the future potential of ammonia in the energy sector. The role of machine learning and artificial intelligence in ammonia decomposition is also emphasized, as these tools open up ways of simulating reaction mechanisms for the exploration of a new generation of high-performance catalysts and reduce trial-and-error approaches.

Keywords: Hydrogen, Renewable energy, Catalysis, Ammonia decomposition, Activity.



1

2

3

Table of Contents

View Article Online

DOI: 10.1039/D4CC06382A

1. Introduction	4
2. Photocatalysis	10
3. Electrocatalysis	18
4. Plasma	26
5. Other	31
6. Predicting NH ₃ decomposition efficiency by machine learning	32
7. Further challenges for ammonia decomposition	34
8. Conclusions and Perspectives	35
Data availability	36
Conflicts of interest	36
Acknowledgements	36
References	37

1. Introduction

The demand for global energy has increased due to a highly energy-intensive lifestyle and the continuing growth of the world's population ¹. Currently, approximately 733 million people globally lack access to electricity, while 2.4 billion people lack clean fuels and modern cooking technologies ². According to the Energy Institute Statistical Review of World Energy 2023, fossil fuels, coal, oil, and natural gas are still the main primary energy sources (82%) ³. There is a broad consensus that fossil fuel reserves, particularly oil, are on the verge of depletion and shortage by the end of this century ⁴. Due to the continuous reliance on fossil fuels, a substantial amount of greenhouse gases (GHGs) such as CO₂, CO, SO₂, NO_x, and volatile organic compounds (mainly CO₂) has been emitted into Earth's atmosphere ⁵⁻⁸. CO₂ is recognized as the primary driver of global warming, with approximately 80% originating from the combustion of fossil fuels within the industrial sector ⁹. To respond to global climate change and meet the Paris Agreement's temperature control goals, there is a worldwide consensus on reducing greenhouse gas emissions toward net-zero carbon emissions ⁹. In this context, China has set a target to reach "peak carbon" by 2030 and "carbon neutrality" by 2060 ¹⁰.

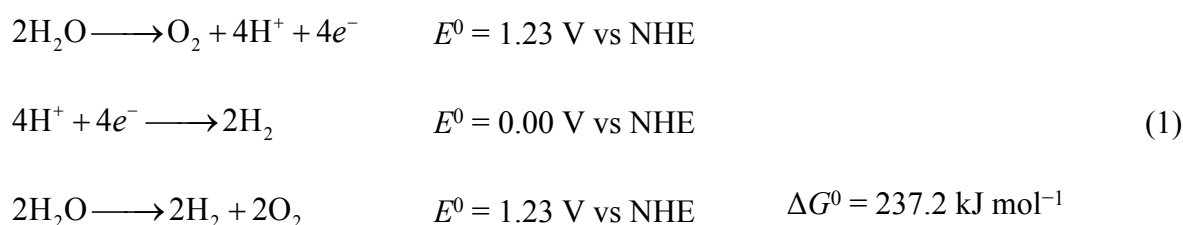
Renewable energy technologies, including solar and wind power, are increasingly achieving cost parity with conventional fossil fuel-based energy sources ¹¹. However, as these energy sources are intermittent and unevenly distributed across the globe, they are still complex to replace traditional energy completely ¹². Therefore, hydrogen (H₂) has been drawn to our attention as a new energy source without pollution or CO₂ emissions.

Hydrogen, with the smallest relative molecular mass, is of significant interest as a secondary energy source due to its high gravimetric energy density (~33 kWh kg⁻¹), which is greater than that of either gasoline or diesel fuel, and its capacity for zero-emission output ^{13, 14}. The U.S. Department of Energy (DOE) initially set hydrogen storage targets in 2009 for applications such as portable power, onboard light-duty vehicles, and material-handling equipment. The

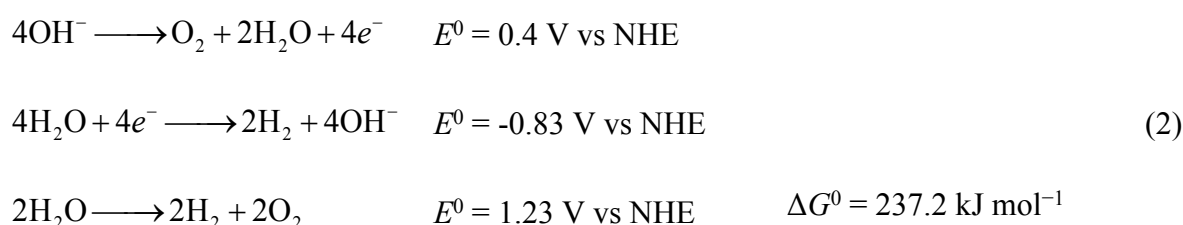


DOE set specific targets for on-board hydrogen storage: 0.030 kg H₂ L⁻¹ and 4.5 wt % for volumetric and gravimetric storage capacities by 2020¹⁵. In addition, China is actively working to increase its production of carbon-neutral hydrogen (green hydrogen) to meet its carbon neutrality goals, which involves water splitting (Eqs. 1-2) to extract hydrogen using electricity generated from renewable sources such as wind and solar energies^{9, 16}. It is expected that till 2025, the specific system targets aim for 1.8 kWh kg⁻¹ system (0.055 kg H₂ kg⁻¹ system), 1.3 kWh L⁻¹ system (0.040 kg H₂ L⁻¹), and \$9 kWh⁻¹ storage system (\$300 kg⁻¹ stored H₂ system).

In acidic solution



In alkaline solution



Currently, hydrogen can be stored in carbon fiber tanks at high pressures (>35 MPa), achieving a gravimetric H₂ capacity of 0.025 kg H₂ kg⁻¹ system at 350 bar¹⁷. Hydrogen can only be liquefied at extremely low temperatures of -253 °C or pressures above 70 MPa that significantly increase the costs associated with the storage and transportation of hydrogen energy⁹. Therefore, the transportation and storage of hydrogen remains a critical barrier, significantly impeding its industrial applications¹⁴.

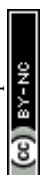


One potential solution to address hydrogen transport issues involves the utilization of liquid or solid hydrogen energy carriers, from which hydrogen is chemically extracted upon arrival. The selection of a hydrogen energy carrier focuses on environmental friendliness, efficiency, ease of handling and transport, and a high hydrogen mass and volume percentage. Given that, methanol and ammonia are frequently discussed as the feasible carriers.⁹

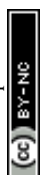
Accordingly, ammonia (NH₃) possesses high H₂ content (17.8 wt%) and a large energy density (3000 Wh kg⁻¹). It has greater volumetric hydrogen density than liquid H₂ (121 kg H₂ m⁻³) and can be liquefied and stored at room temperature, facilitating the transportation and storage, particularly in the liquid phase, as NH₃ gas is liquefied under a pressure of 8.5 MPa at 20 °C^{18, 19}. Notably, hydrogen produced through ammonia decomposition typically contains fewer impurities compared to hydrogen derived from hydrocarbons (like methanol)²⁰.

Ammonia decomposition has been mainly investigated since the 19th century¹⁸. In 1904, Perman and Atkinson reported that complete decomposition of ammonia is not achievable below 1100 °C. They also noted that the degree of decomposition depends significantly on the nature of the surface in contact with the ammonia, particularly the catalysts involved²⁰. To date, various metals, alloys, and their compounds (such as oxides and nitrides) have been extensively studied as active catalysts for NH₃ decomposition. Given that ammonia decomposition is the exact reverse of industrial ammonia synthesis from nitrogen and hydrogen, the microkinetic principle suggests that catalysts effective for NH₃ generation should, in theory, facilitate ammonia decomposition. However, the catalytic activity trends differ significantly between the two processes due to their opposing reaction pathways and targeted products²¹.

Prior to 1990, Fe-based catalysts attracted significant interest, however, in the past decade, research has increasingly shifted toward noble metal catalysts, with growing attention on metal nitrides, carbides, and alloys as active components for the decomposition reaction²². Till now,



1 various monometallic systems based on non-noble metals have been investigated for hydrogen
2 production from ammonia. Over the last decade, the catalytic decomposition of NH_3 over
3 catalysts such as platinum (Pt), palladium (Pd), ruthenium (Ru), and rhodium (Rh) has gained
4 a lot of attention in substitution of iron¹⁸. While, these metals show outstanding activities, their
5 large-scale applications significantly increase the cost, which is a substantial drawback²³. To
6 tackle this issue, transition metal carbides (MoC_x , VC_x , WC_x , and FeC_x) and nitrides (MoN_x ,
7 VN_x , and WN_x), along with zirconium oxynitride have been recruited. Amidst those,
8 molybdenum nitride and tungsten carbide have received the most attention in ammonia
9 decomposition studies. Notably, these catalysts are generally evaluated under conditions
10 relevant not only to hydrogen production but also to gasification mixture clean-up²⁴. For
11 bimetallic catalysts, several studies have been explored, including Ni–Pt, Ni/Ru, Pd/Pt/Ru/La,
12 and Fe– MO_x ($\text{M} = \text{Ce}$, Al , Si , Sr , and Zr). However, a key challenge for bimetallic catalysts
13 remains the structural stability of these catalysts under reaction conditions, particularly
14 concerning metal segregation. This could lead to increased energy consumption, creating
15 potential obstacles for the decomposition of NH_3 ²⁵. Given that enhanced metal interactions
16 appear to contribute to higher catalytic activity, optimizing preparation methods and selecting
17 appropriate metal salts could offer promising strategies for improving performance²⁶.
18 Research has shown that alloying strategy can play a crucial role in facilitating ammonia
19 decomposition reaction to their monometallic counterparts by improving the catalytic
20 performance of catalysts^{25, 27}. In this area, a broad range of alloy systems has developed,
21 including Co alloys with Ni²⁸, Re²⁹ and Ce³⁰, Ni alloys with Co, Fe, and Cu³¹, Ru–Ni³², Cu–
22 Zn³³, etc. These findings demonstrate that alloy-based catalysts could provide a more cost-
23 effective alternative while preserving—or even exceeding—the catalytic efficiency of noble
24 metals³⁴. However, choosing the right elements and appropriate stoichiometric composition
25 remains a significant challenge for NH_3 decomposition over alloyed catalysts to ensure both



optimal activity and long-term stability³⁵. Therefore, one of the most significant challenges in the preparation of hydrogen from ammonia decomposition is to customize an effective catalyst that is energy efficient, highly selective, scalable, and affordable, providing a stable rate of decomposition at low temperatures³⁶.

Recent researches have shifted focus from Ru-based catalysts to alternative transition metal (TM) and TM-free catalysts. Among these, alkali amides and imides, particularly lithium-based compounds such as LiNH₂ and Li₂NH, have demonstrated a significant reduction in activation barriers by stabilizing M–N bond intermediates. Theoretical studies further highlight the importance of surface disorder dynamics in non-stoichiometric lithium amide compounds (Li_{2-x}(NH₂)_x(NH)_{1-x}) for TM-free catalysis, suggesting mechanistic differences from TM-based systems. Similar to TM-free NH₃ synthesis catalysts, lithium amides/imides exhibit catalytic activity for ammonia decomposition both with and without transition metals. Notably, addition of TM to LiNH₂ enhances NH₃ conversion at 440 °C from 54% to 86%, in which catalytic performance was also influenced by ammonia flow rates³⁷. Table 1 provides a summary of the most effective heterogeneous catalysts used for the thermal decomposition of ammonia.

Table 1. The most effective heterogeneous catalysts utilized for the decomposition of ammonia¹⁸.

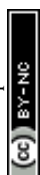
Catalyst	Temperature (°C)	Conversion (%)	TOF (1/s)	Ref.
Ni/MgAl ₂ O ₄ – LDH	600	88.7	2.18	38
Co/NC-600	500	80		39
Ru/SmCeO _x	400	74.9	25.81	40
35Co/BHA	500	87.2		41
2.5Ru/10 C-rGO	400	96	75.4	42



CoRe _{1.6}	500	~90		29 View Article Online DOI: 10.1039/D4CC06382A
K ⁺ -Fe/C	470	20	~0.5	43
Ru/Al ₂ O ₃	580		6.85	44
20Co–10Ni/Y ₂ O ₃	550	71.2		45
Co-containing CNTs	700	~100		46
Ni-10/ATP	650	64.3		47
α-FeO ₂ O ₃ -50 @pSiO ₂	800	100		48
10%Co/MWCNTs	600		8.15	49
Ru/La _{0.33} Ce _{0.67}	450	91.9	11.4	50
Ni ₅ Co ₅ /SiO ₂	550	76.8		28
5CMLa-5	550	82.7		51
1%K-Co/SiC	350	33.1	9.3	52
Pr-Ni/Al ₂ O ₃	550	~90		53

From this perspective, significant progress has been made in recent years in developing alternative methods, with a focus on reducing reaction temperatures. This advancement aims to lower energy consumption while enhancing hydrogen production efficiency⁵⁴. Until now, electric currents, electron beams, ions, microwaves, plasma, and solar energy are alternative approaches to provide new feasible solutions for ammonia decomposing (Fig. 1)⁵⁵. Although numerous reviews have been published on the progress of ammonia decomposition, the literature has overlooked assessing the different approaches for green H₂ generation from NH₃ and the subsequent technical barriers to achieving a futuristic fuel and sustainable energy vector.

Hence, this review aims to summarize and analyze previously reported green ammonia cracking aspects, such as photocatalysis, electrocatalysis, and other approaches, as well as their



mechanisms of catalytic activity. Furthermore, the influences of recent revolution in data science, artificial intelligence (AI), and machine learning (ML), on the discovery of novel catalysts for the NH_3 -to- H_2 reaction are evaluated. Finally, based on the literature and our experience, the current challenges and future perspectives for achieving the rapid commercialization of NH_3 decomposition and green H_2 production are discussed.

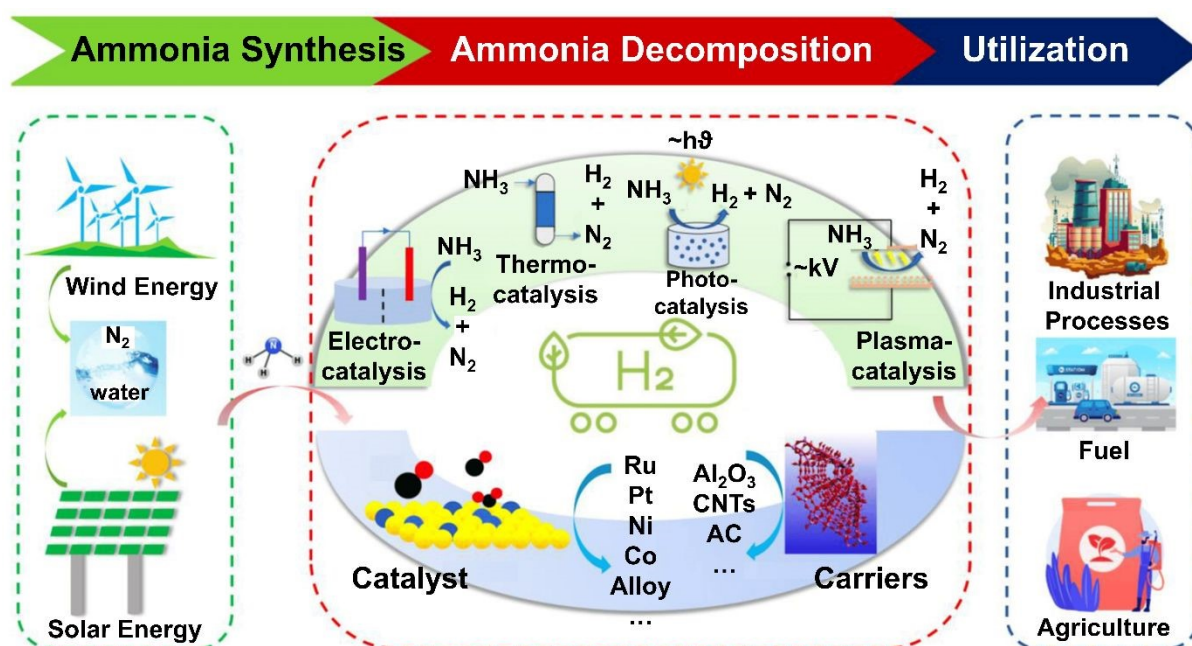


Figure 1. The status of hydrogen generation from ammonia decomposition. This figure was adapted with the permission from Ref. ⁵⁶. Copyright 2023, MDPI.

2. Photocatalysis

In recent decades, the study of photocatalytic ammonia decomposition reactions has garnered significant attention due to their potential applications in energy production, driven by growing concerns over environmental impact and the increasing demand for energy amid dwindling nonrenewable fossil fuel resources ¹⁹. The photocatalytic decomposition of NH_3 into N_2 and H_2 presents a viable approach, as it can be conducted at room temperature using recyclable catalysts and allows facile control of light exposure via a switch. Moreover, utilizing sunlight



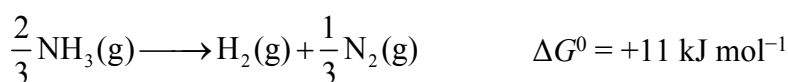
for ammonia decomposition via photocatalysis represents an artificial photosynthetic reaction that proceeds under alkaline conditions ⁵⁶.

Fundamentally, photocatalysis involves a redox reaction that utilizes photogenerated electrons (e^-) and holes (h^+) from semiconductors. The overall process unfolds in three key stages. First, photons excite charge carriers, initiating the reaction. Next, these charges are separated and migrate across the photocatalytic surface. Finally, the photo-activated charge carriers drive catalytic reactions at the surface, facilitating water oxidation and reduction. These steps are elaborated in Eqs. 3-12 ⁵⁷⁻⁶².

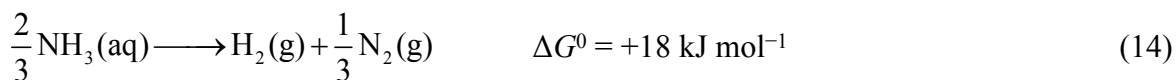


From a thermodynamic perspective, the production of hydrogen through the decomposition of ammonia (Eqs. 13-14) is more favorable compared to splitting water ^{63, 64}.

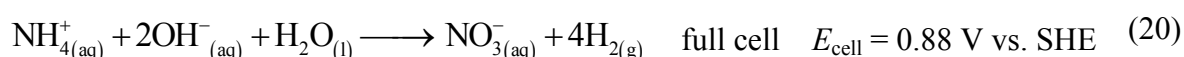
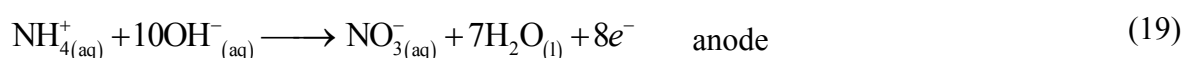
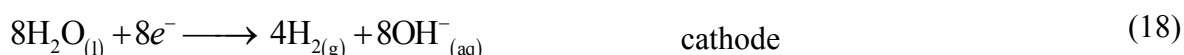
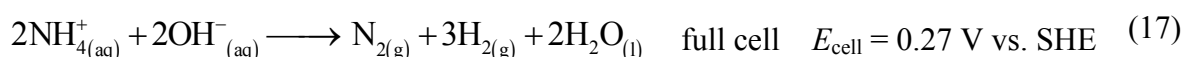
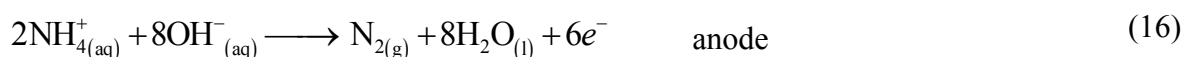




View Article Online
DOI: 10.1039/D4CC06382A

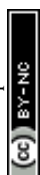


Notably, photocatalytic reactions involving ammonia are feasible only when the reduction and oxidation potentials of ammonia fall between the semiconductor's conduction band (CB) and valence band (VB) potentials. During this process, various nitrogen-containing products such as N_2 , NO_2^- , NO_3^- , and NO_x can be formed owing to their closely related redox potentials. The specific potentials of these reactions are detailed in Eqs. 15-20⁶⁵ and Fig. 2a. Technically, ammonia decomposition can yield varying quantities of different products depending on several reaction parameters such as pH, temperature, initial ammonia or O_2 concentration, and the presence of trapping or sacrificial agents. For an effective photocatalytic degradation of ammonia, the photogenerated electrons and holes on the semiconductor surface must possess appropriate reduction and oxidation capabilities. These enable reactions with species adsorbed on the catalyst surface, such as O_2 , NH_4^+ , NO_2^- , and NO_3^- , facilitating the generation of free radicals or diverse products.



Furthermore, the photocatalytic decomposition of ammonia typically ceases under acidic conditions, suggesting that H^+ ions impede the transformation of ammonia into NH_2 free radicals. As the pH increases, ammonia is likely to react with surrounding oxygen, forming NO_2^- , NO_3^- , and other nitrogen oxides and adversely affecting hydrogen production. However, many photocatalysts currently face significant challenges with carrier recombination and poor light-harvesting efficiency. Consequently, the development of more effective photocatalytic materials remains crucial for the advancement of ammonia treatment through photocatalytic technologies ⁶⁶.

To date, only a group of photocatalysts, such as TiO_2 , ZnO , ZnS , Mo_2N , graphene, and their metal-loaded hybrid materials, have been found effective in decomposing aqueous ammonia solutions ⁵⁶. However, their hydrogen production rate, capped at $15.56 \mu mol g^{-1} min^{-1}$, remains insufficient to satisfy practical application requirements ⁶⁷. To address this shortcoming, Utsunomiya *et al.* ¹⁹ investigated the photocatalytic performance of Ni/TiO_2 catalysts in ammonia decomposition and explored the mechanism of NH_3 breakdown by proposing three distinct reaction pathways (Fig. 2b). These pathways involved the formation of N_2 and H_2 through intermediates radicals: route 1 entailed the formation of NH radicals via the removal of one hydrogen atom from two NH_2 radicals; route 2 involved the direct coupling of adjacent NH_2 radicals to form NH_2-NH_2 ; and route 2', where NH_2-NH_2 formation occurred through the interaction of H_2N-NH_3 . The activation energies for routes 1 and 2 were determined to be 236 $kcal mol^{-1}$ and 74.8 $kcal mol^{-1}$, respectively, with route 2 being more energetically favorable. Additionally, the pathways for N_2 and H_2 formation via NH_2-NH_2 coupling were further delineated into route 2, which involved the coupling of NH_2 radicals to form H_2N-NH_2 , and route 2', where NH_2 interacted with an NH_3 molecule in the gas phase. Alternatively, beyond photocatalysis, solar heating catalysis demonstrates the highest efficiency in sunlight utilization (approaching 100%) and can achieve temperatures up to 400



1 °C. This facilitates the heating of catalysts for thermocatalysis under natural solar irradiation.

2 In the context of solar-powered ammonia decomposition, cobalt-based catalysts are preferred

3 due to their abundance and effectiveness⁶⁷. Yuan *et al.*⁶⁷ developed a catalyst by immobilizing

4 single atoms of cobalt on cerium dioxide nanosheets (SA Co/CeO₂) (Figs. 2c and 2d) for

5 photocatalytic degradation of ammonia in tubular reactor at low temperatures (Fig. 2e). As can

6 be seen in Fig. 2f, integrated with a custom-built TiC/Cu-based solar heating device, the SA

7 Co/CeO₂ demonstrated a stable hydrogen generation rate of 2.7 mmol g⁻¹ min⁻¹ under 2 solar

8 irradiation, which is 572 times more effective than traditional weak sunlight-driven ammonia

9 decomposition. The hydrogen produced was found to be sufficiently pure to power a hydrogen

10 fuel cell without further purification directly. Theoretical calculations revealed that SA

11 Co/CeO₂ significantly lowers the energy barrier for nitrogen binding during ammonia

12 decomposition, thereby enhancing the reaction's progress (Fig. 2g).



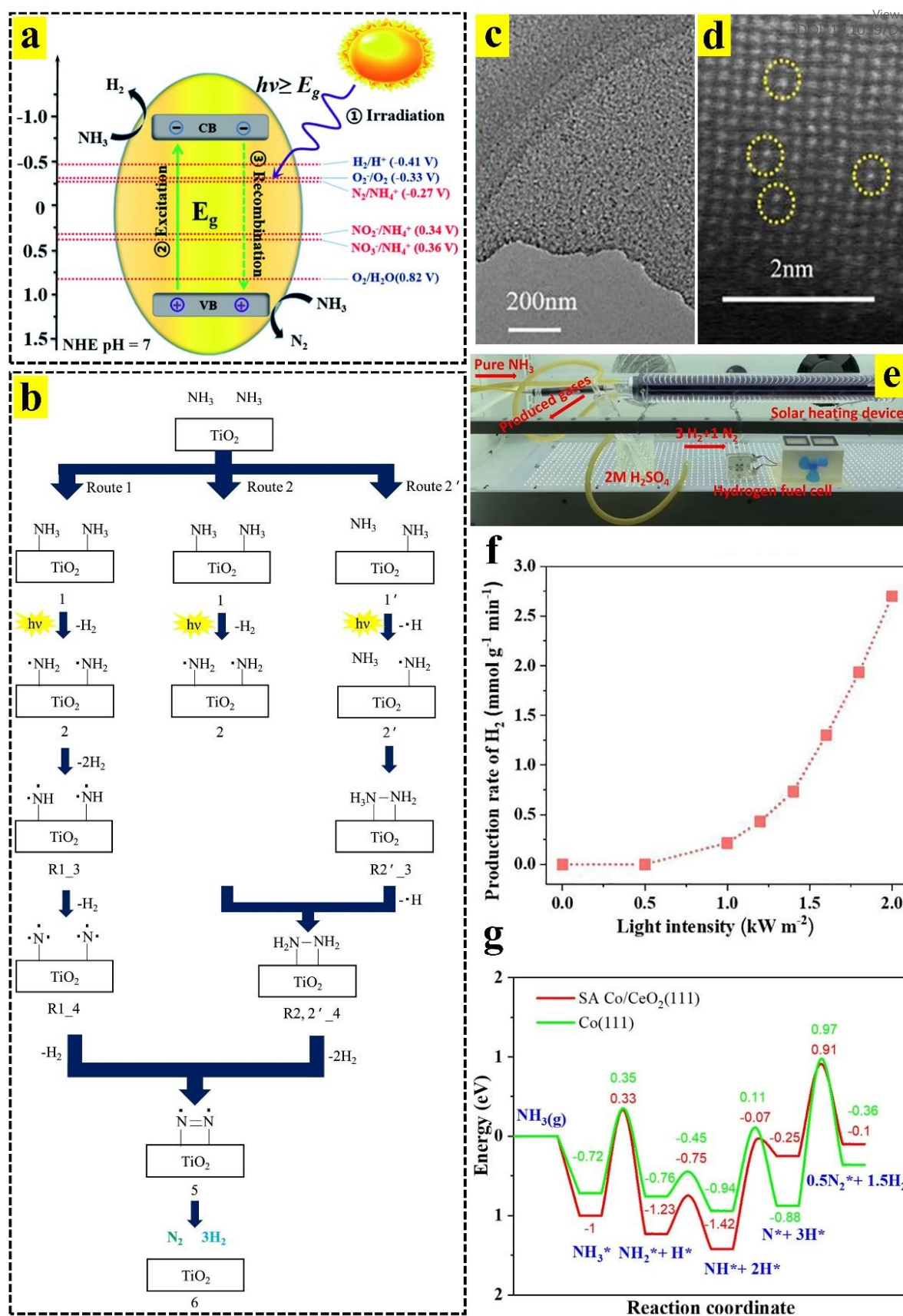


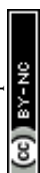
Figure 2. (a) Schematic process of photocatalytic NH_3 decomposition. This figure was adapted with the permission of Ref. ⁶⁸. Copyright 2020, Royal Society of Chemistry. (b) Proposed



1 reaction mechanism for NH_3 decomposition to N_2 and H_2 on TiO_2 photocatalyst. This figure
2 was adapted with the permission of Ref. ¹⁹, Elsevier. (c) TEM image and (d) HAADF-STEM
3 image of SA Co/CeO₂. (e) Photograph of SA Co/CeO₂ loaded in a novel solar heating device
4 to drive hydrogen fuel cell under 2 solar irradiation. (f) H_2 production rate from NH_3
5 decomposition by SA Co/CeO₂. (g) Energy profiles for NH_3 decomposed as H_2 and N_2 on SA
6 Co/CeO₂ (111) and Co (111) surfaces. These figures were adapted with the permission of Ref.
7 ⁶⁷. Copyright 2023, Elsevier.

8
9 Moreover, Lin *et al.* ⁶⁹ employed a straightforward nebulization-coating technique to
10 immobilize a wide array of single-atom transition metals (TMs: Co, Mn, Fe, Ni, Cu) onto
11 microporous carbon nitride (MCN) (Fig. 3a), creating catalyst panels designed for solar-light-
12 driven photocatalytic gaseous ammonia splitting (Fig. 3b). Under ambient conditions, the
13 optimized Ni-MCN demonstrated a hydrogen production rate of $35.6 \mu\text{mol g}^{-1} \text{h}^{-1}$,
14 significantly outperforming pure MCN (by approximately 14-fold) and other composite
15 alternatives (Fig. 3c). This enhanced photocatalytic activity and photocurrent response (Fig.
16 3d) can be attributed to the presence of Ni-N₄ sites, which enhance the optical properties,
17 expedite charge carrier separation/transfer, and improve the kinetics of ammonia splitting on
18 the catalysts. Regarding Fig. 3e, the Ni site on MCN is the most favorable for NH_3 splitting
19 among all these TMs due to its lowest free energy increase in the potential-determined step
20 (PDS).

21 In another study, Dzibelov'a *et al.* ⁷⁰ utilized an ultrasound-supported exfoliation technique to
22 anchor ruthenium oxide nanoparticles onto 2D hematene ($\alpha\text{-Fe}_2\text{O}_3$) (Fig. 3f) for the
23 decomposition of an aqueous ammonia solution into hydrogen and nitrogen under visible light
24 irradiation. Experimental results demonstrated that with an optimal ruthenium dosage of 0.5
25 wt%, the Ru-hematite, after 24 hours, achieved a hydrogen yield that was 2.5 times higher than



that of pure hematene (Fig. 3g), attributed to the enhanced generation of electrons and holes (Fig. 3h). Moreover, without any cleaning interventions, the Ru-hematite photocatalyst exhibited only an 11% reduction in photocatalytic activity after five consecutive runs, suggesting its suitability for practical applications.

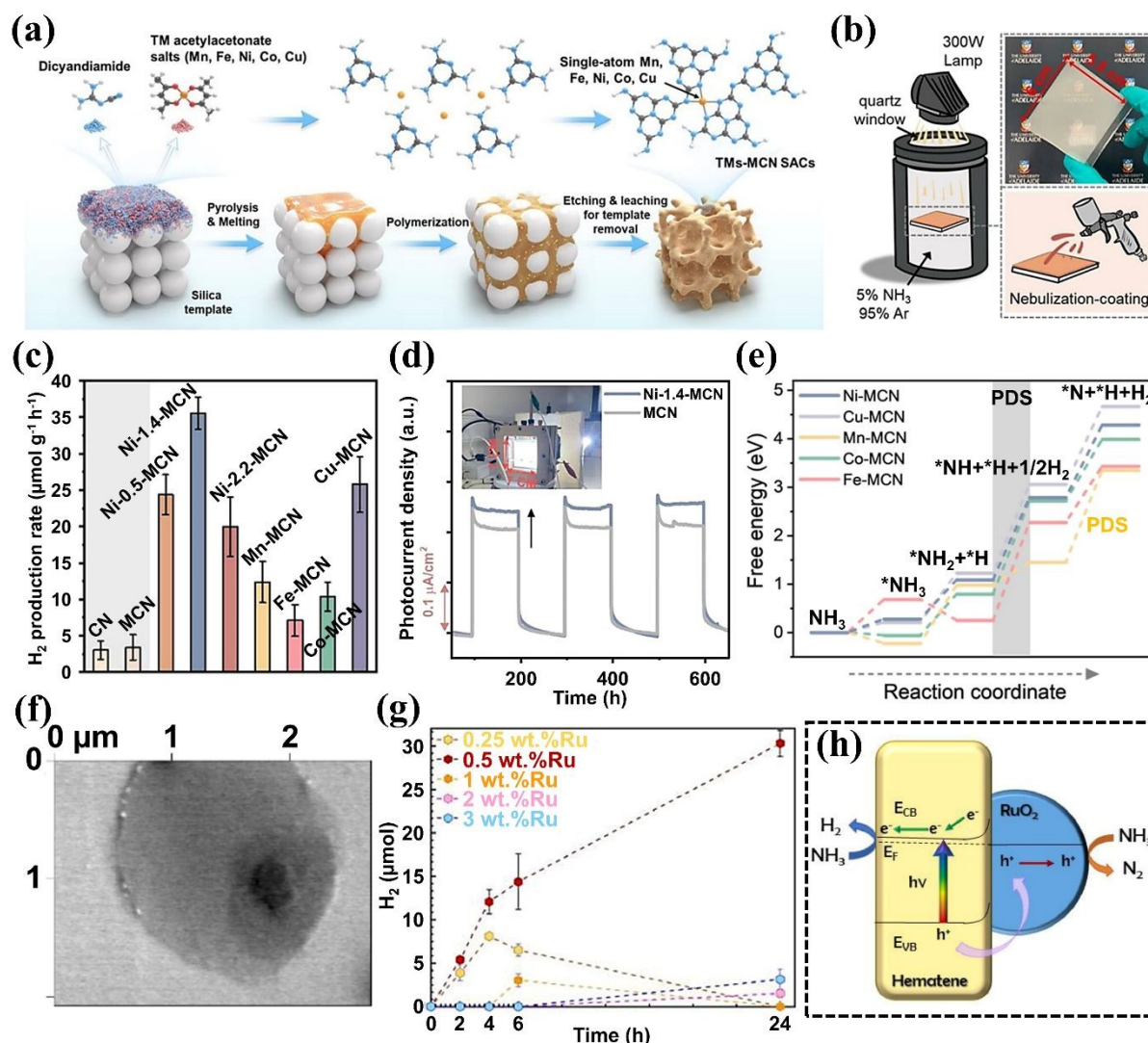


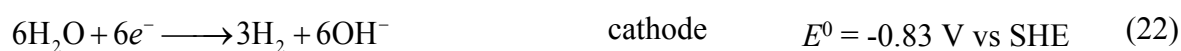
Figure 3. (a) Schematic of the synthesis procedure of TMs-MCN SACs. (b) Illustration of the reaction system and nebulization-coating method for fabricating TMs-MCN panels. (c) Rates of H₂ production by CN, MCN, and Ni-MCNs with different Ni loadings and TMs MCNs (TMs = Mn, Fe, Co, Ni, Cu, with a similar loading percentage of ~1.4 wt %). (d) Photocurrent responses of MCN and Ni-1.4-MCN (inset: picture of the large-sized cell). (e) Energy profiles



for the reaction process. These figures were adapted with the permission of Ref. ⁶⁹ Copyright 2023, American Chemical Society. (f) Correlative probe and electron microscopy image of hematene sheet. (g) Decomposition of ammonia over Ru-hematene samples to optimize weight loading of Ru. (h) Schematic mechanism of ammonia decomposition by Ru-hematene photocatalyst. These figures were adapted with the permission of Ref. ⁷⁰. Copyright 2023, Elsevier.

3. Electrocatalysis

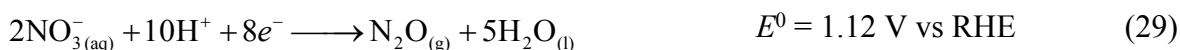
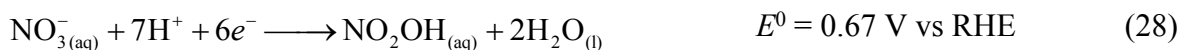
Recently, hydrogen generation through electrochemical reactions, such as ammonia decomposition by electrocatalysis at moderate temperatures, has attracted more attention.⁷¹ However, ammonia decomposition faces challenges such as high overpotentials, unfavorable thermodynamics, and slow reaction kinetics ⁷². Based on the different existing states of NH₃, electrochemical ammonia decomposition can be categorized into the electrolysis of (i) aqueous ammonia solution, or (ii) liquid ammonia. In the electrolysis of alkaline aqueous ammonia solutions, NH₃ undergoes oxidation in the existence of OH⁻ ions at the anode (Eq. 21) ⁷³, whereas H₂O can be reduced at the cathode (Eqs. 22 and 23) ^{71, 74, 75}.



In 2002, Zisekas *et al.* ⁹ utilized silver as the reactor electrode to conduct the first tests on hydrogen production via electrocatalytic decomposition of ammonia. These tests demonstrated that NH₃ conversion efficiency ranged between 25–35% at temperatures of 773–873K, indicating that reactor temperatures remained relatively high. It is well accepted that the energy



1 density of hydrogen in liquid ammonia [NH₃(l), 3.6 kW h L⁻¹] is significantly higher compared
 2 to that in alkaline aqueous ammonia solution [NH₃(aq), 1.0 M, 0.1 kW h L⁻¹]. Fundamentally,
 3 the electrolysis of liquid ammonia differs from that of aqueous ammonia solutions, as both the
 4 anodic and cathodic half-reactions in liquid ammonia avoid the excessive oxidation of
 5 ammonia that typically occurs in the presence of water ⁷¹. Furthermore, the gravimetric
 6 H₂ density is as low as 6.1 mass % according to its solubility to water, 34.2 mass % at 20 °C
 7 ⁷⁶. Thus, Hanada *et al.* ⁷⁷ evaluated the direct electrolysis of liquid ammonia, where alkaline
 8 metal amides (MNH₂, M = Li, Na, K) were utilized as the supporting electrolyte. Amides such
 9 as LiNH₂, NaNH₂, KNH₂, and N, N-dimethylformamide have enabled the electrolysis of liquid
 10 ammonia. This process was conducted at exceptionally low temperatures, ranging from -70 to
 11 -65°C, using pure platinum electrodes ⁷⁸.
 12 Moreover, during electrocatalytic reaction, NH₃ can be converted aqueous to NO₃⁻ and then to
 13 products such as HNO₂, NO, NH₂OH, NH₃, N₂O, and N₂ (Eqs. 24-30). Generated nitrogen is
 14 benign and easily separable, and is the most stable nitrate reduction product with a standard
 15 redox potential (*E*⁰) of 1.25 V vs. RHE ⁷².

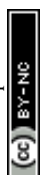


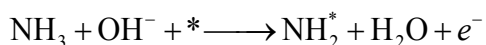
17



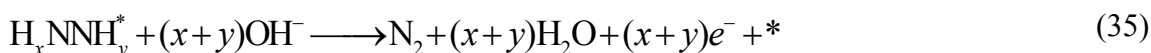
Technically, the electrocatalytic decomposition of ammonia encompasses two primary phases: (i) the ammonia oxidation reaction (AOR) and (ii) the hydrogen evolution reaction (HER). An effective high-efficiency electrocatalyst should be capable of catalyzing both AOR and HER at a low potential ³⁶. Despite its potential, the activity level of AOR is insufficient for low-temperature operations. AOR integrates more easily with fuel cell technologies and provides a more effective method for hydrogen generation than water electrolysis, which represents the second most common hydrogen production method and accounts for approximately 4% of global hydrogen production. Water electrolysis, which is not thermodynamically favored, theoretically necessitates applying a voltage as high as 1.23 V to break down highly stable water molecules, requiring about 180 MJ of energy to produce 1 kg of H₂. In contrast, AOR has a significantly lower energy requirement of approximately 33 MJ per kg of hydrogen generated ⁷⁹.

Research has demonstrated that the electrocatalytic activity for ammonia oxidation correlates with the properties of surface materials. The catalyst remains active when intermediate NH_x species are present but becomes inhibited when strongly binding nitrogen species are formed ⁸⁰. In this context, the widely accepted mechanism was proposed by Gerischer and Mauzer in 1970, with the fundamental steps detailed in Eqs. 31-35. Briefly, NH₃ can be deprotonated in the presence of hydroxyl ions in Eqs. 31-33, producing water molecules while simultaneously releasing an electron at each step. N* adatoms (formed in Eq. 33) are surface poisons because of a typically large kinetic barrier for N–N bond formation and release nitrogen. Thus, adsorbed NH_x (and NH_y) species can interact with one another to form an N–N bond, subsequently generating an H_xNNH_y species (Eq. 34). Regarding the Gerischer–Mauzer mechanism, these species are then deprotonated to N₂, which desorbs from the surface; however, the identity of the NH_x and NH_y species that react to form the N–N bond remains in dispute (Eq. 35) ⁸¹.





View Article Online
DOI: 10.1039/D4CC06382A



The catalytic activity can be substantially enhanced when a portion of the metal is utilized as an electrode by applying a current or potential between the catalyst and a counter electrode deposited on the solid electrolyte³⁶. To date, a diverse range of materials, such as noble metals, metal oxides, and non-metals, have demonstrated high catalytic activity for ammonia electro-oxidation. Notably, Pt has emerged as the most effective electrocatalyst for this reaction. However, most ammonia electro-oxidation systems necessitate strong alkaline media (such as NaOH), leading to rapid deactivation and poisoning of Pt catalysts, as well as oxygen evolution and NO_x production. Under strongly alkaline conditions, electrodeposited Pt electrodes and nanotubes have effectively oxidized ammonia into hydrogen⁷⁸.

In this context, Herron *et al.*⁸¹ examined AOR efficiency on various face-centered cubic (fcc) metals (Au, Ag, Cu, Pd, Pt, Ni, Ir, Co, Rh, Ru, Os, and Re) using density functional theory (DFT) calculations. They reported that Pt exhibited the most promising catalytic activity, followed by Ir and Cu, due to its low onset potential (Figs. 4a and 4b). It was found that adsorbed NH₂ was the dominant intermediate, facilitating the preferred N–N bond formation both kinetically and thermodynamically (Fig. 4c). In another study, Zhong *et al.*⁸⁰ investigated catalytic electro-oxidation of liquid ammonia using transition metal dimers (Fe₂, Co₂, Ru₂, Rh₂, and Ir₂) anchored on graphite-carbon nitride monolayers (TM₂@g-CN). Their findings reinforce the mechanism proposed by Gerischer and Mauzer, where N–N bond formation is



1 facilitated by hydrogenated NH_x species rather than N adatoms (Fig. 4d). Catalytic activity
2 studies demonstrated that Fe, Co, Ru, Rh, and Ir anchored in g-CN monolayers are
3 exceptionally promising AOR catalysts due to their low limiting potentials of -0.47 , -0.5 ,
4 -0.48 , -0.52 , and -0.48 V, respectively. Among them, $\text{Ir}_2@\text{g-CN}$, as a bifunctional catalyst
5 for electrocatalytic NH_3 decomposition, showed low energy barriers of 0.48 eV and 0.20 eV
6 for AOR (Fig. 4e) and HER (Fig. 4f), respectively. It was found that modulating TM atoms
7 with varying d-electron numbers allows for tuning the d -band center (ϵ_d) of TM atoms on
8 $\text{TM}_2@\text{g-CN}$, providing a predictive measure for AOR performance and offering theoretical
9 guidance for designing advanced AOR electrocatalysts.

View Article Online
DOI: 10.1039/D4CC06382A



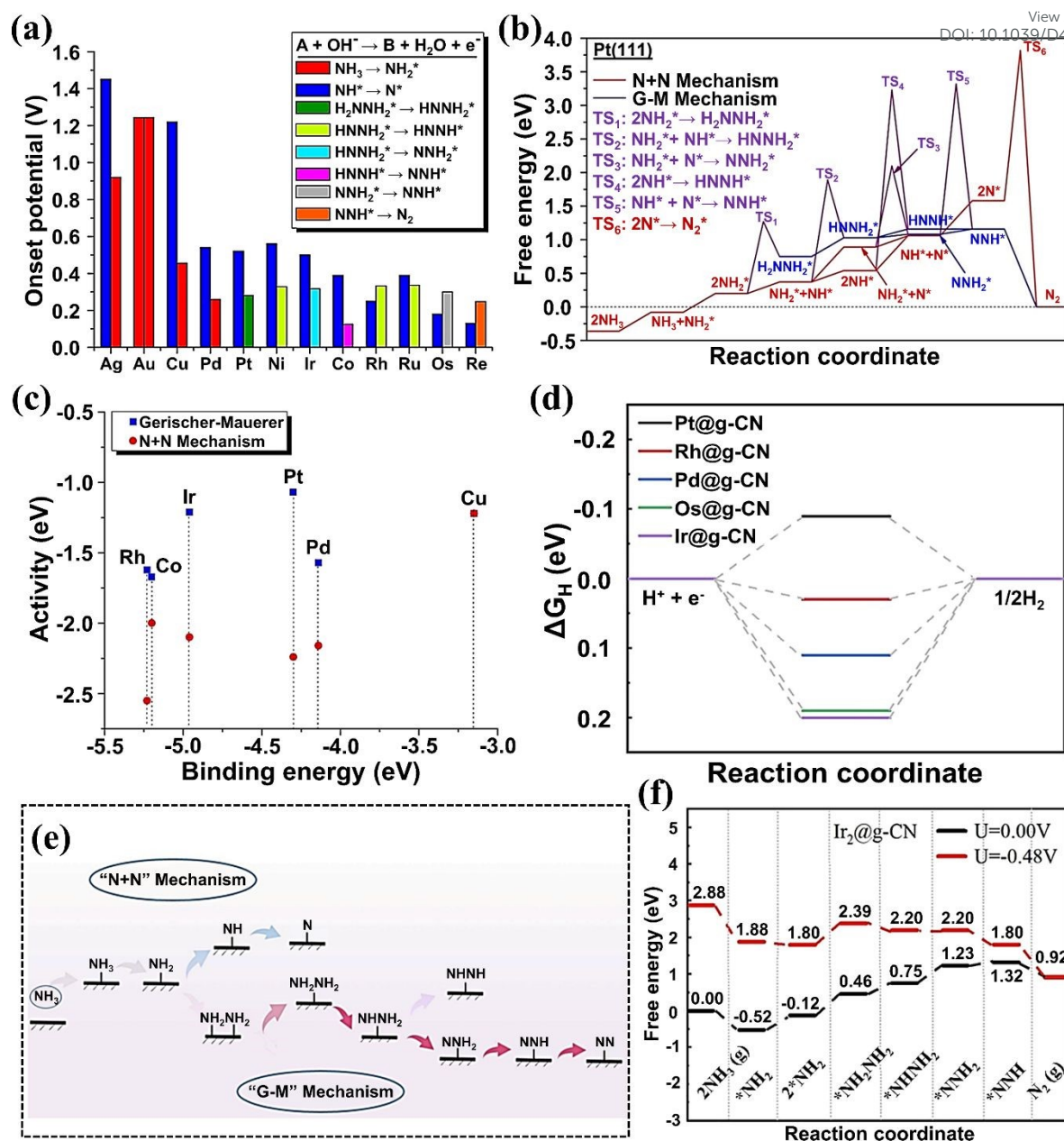
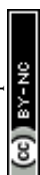


Figure 4. (a) Estimated onset potential for close-packed facets of transition metals. (b) Activity as predicted by Sabatier analysis for both mechanisms at 0 V_{RHE}. (c) Free-energy diagram for ammonia electro-oxidation on Pt(111) at 0 V_{RHE}. These figures were adapted with the permission of Ref. ⁸¹. Copyright 2015, American Chemical Society. (d) Proposed mechanism for AOR on TM₂@g-CN. (e) The calculation free energy diagram of AOR through the Gerischer–Mauerer mechanism on Ir₂@g-CN at different applied potentials. (f) The calculated



1 free energy diagram of the HER on $\text{TM}_2\text{@g-CN}$ samples. These figures were adapted with the
2 permission of Ref. ⁸⁰. Copyright 2023, Elsevier.

3
4 In Modisha's study ⁸², decomposition of ammonia using a Pt-Ir electrocatalyst was investigated
5 in a potassium hydroxide (KOH, 5M) solution (Fig. 5a). This research demonstrated that the
6 current density of ammonia electro-oxidation reaction rose at high temperature and ammonia
7 concentration, achieving a peak ammonia conversion of 78% at 2300 ppm (Fig. 5b). From Fig.
8 5c, the highest hydrogen flow rate recorded was 25 L h^{-1} , with an associated energy
9 consumption of $1.6 \text{ Wh L}^{-1} \text{ H}_2^{-1}$. The purity of hydrogen, as determined by gas
10 chromatography, was found to be 86%. Moreover, Dong *et al.* ⁸³ synthesized five types of
11 electrocatalysts, including Pt-Black, Rh, Pt-Ir, Rh-Pt, and Rh-Pt-Ir alloys, aimed at reducing
12 the overpotential of the anode reaction for ammonia cracking (Fig. 5d). These alloys were
13 electrochemically evaluated for their efficacy in ammonia decomposition in the presence of
14 NH_4Cl . The trimetallic Rh-Pt-Ir and the bimetallic Pt-Ir, as well as the Rh-contained alloy
15 electrodes, demonstrated enhanced activity and reduced deactivation. Notably, the Rh-Pt-Ir
16 alloy anode (Fig. 5e) exhibited the highest electrocatalytic activity, achieving the lowest
17 minimum potential (E_{min}) of approximately 0.47 V and the highest current density of 46.9 mA
18 cm^{-2} at 2.0 V (Fig. 5f). The results of this research reflect that the energy required for hydrogen
19 generation from the electrolysis of liquid NH_3 can be significantly lowered through strategic
20 selection and compositional optimization of alloy catalysts.



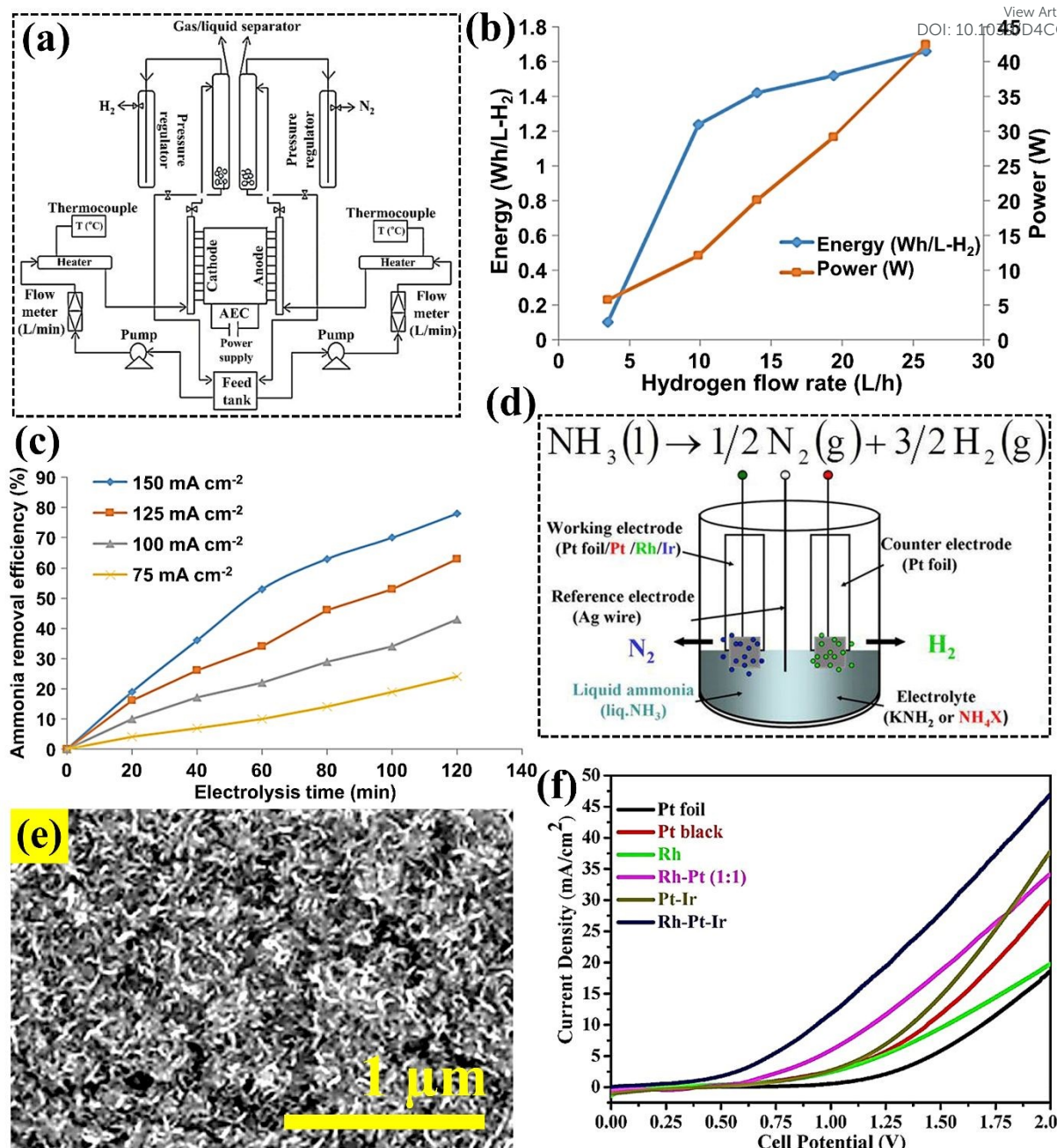


Figure 5. (a) Schematic representation of ammonia electrolysis process for hydrogen production. (b) Volumetric hydrogen generation rates and corresponding required energy and power input (cell retention time (Rt): was 12.5 min, 2000 ppm NH_3 in 5 M KOH at 55 $^{\circ}C$). (c) Ammonia decomposition efficiency as a function of time and current density. These figures were adapted with the permission of Ref. ⁸². Copyright 2016, Elsevier. (d) Schematic electrolysis of liquid ammonia using different ammonium salt electrolytes with the reference electrode. (e) SEM image of the freshly prepared Rh-Pt-Ir electrocatalyst. (f) Cyclic

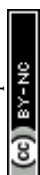


voltammetry curves of NH_3 (l) with 1 M NH_4Cl in two-electrode system. These figures were adapted with the permission of Ref. ⁸³. Copyright 2016, Elsevier.

4. Plasma

As mentioned earlier, significant research efforts have been directed toward developing alternative energy supply methods for ammonia decomposition. These methods include the use of electric currents ⁸⁴, electron beams ⁸⁵, microwaves ⁸⁶, and plasma ⁸⁷, which offer higher conversion rates at lower temperatures compared to traditional thermal catalysis. Among them, there has been a notable shift towards exploring non-thermal plasma (NTP) for catalytic ammonia decomposition at low temperatures. This approach potentially enhances the response time and modularity of ammonia-based hydrogen production systems, thereby improving their applicability in sectors like transportation ⁸⁸.

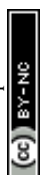
Plasma is generally defined as a state of gas where the atoms are partially or fully ionized, maintaining overall electrical neutrality, containing a large number of highly energetic electrons and reactive species (e.g., excited molecules, atoms, ions, and radicles) (Figs. 6a-6c) ^{9, 89, 90}. It was found that integrating non-thermal plasma with a catalyst can significantly modify the catalytic reaction pathway, leading to enhanced selectivity or reaction rates through the interaction of plasma, reactant, and catalyst ⁸⁹. Notably, the H_2 energy yield from the plasma catalysis method is nearly five times greater than that achieved through thermal catalysis. This indicates that plasma catalysis substantially enhances the economic efficiency of hydrogen production from ammonia ⁹. In 2006, research on the impact of dielectric barrier discharge plasma on ammonia decomposition revealed that using a commercially available bulk Fe-based catalyst significantly increased NH_3 conversion rates. Specifically, NH_3 conversion escalated from 7.4% to 99.9% when the Fe-based catalyst was positioned within a plasma zone at 410 °C ⁹¹. In this context, the researchers further optimized the ammonia decomposition process by



utilizing low-temperature plasma, either using high-performance catalysts or by identifying optimal reaction conditions.

In 2015, Wang *et al.*⁹¹ conducted a comparative study on the efficiencies of hydrogen generation from ammonia using both thermal and plasma catalysis methods over different low-cost metal catalysts (Fe, Co, Ni, Cu) on fumed SiO₂ support (Fig. 6d). The results indicated that the NH₃ conversion strongly depends on the metal–N bond strengths and on the relative dielectric constant of the support in the plasma reaction. It was observed that the moderately strong Co–N bonds can be expected to improve the plasma–catalyst synergy, thus leading to higher NH₃ conversions (Fig. 6e). Notably, the relative dielectric constant (ϵ_d) of the support can efficiently contribute to plasma-catalytic NH₃ decomposition performance. As shown in Fig. 6f, a support with a small ϵ_d facilitates plasma-catalytic ammonia decomposition. Technically, plasma gas discharge can rapidly heat the reaction/catalyst, enhancing the energy efficiency of hydrogen production. Additionally, plasma has been shown to facilitate the rate-limiting step by accelerating the recombinative desorption of N_{ad} from the catalyst bulk structure⁸⁹. In another study, the effects of varying discharge zone lengths on the efficiency of plasma-catalytic ammonia decomposition at a set discharge frequency were investigated. The research revealed that doubling the discharge zone length from 3.0 cm to 3.5 cm at a frequency of 10 kHz resulted in a twofold increase in NH₃ conversion efficiency⁹. Consequently, these findings indicate that non-thermal plasma and catalysts can synergistically interact to efficiently convert NH₃ to H₂ under mild conditions. However, despite the potential of plasma-catalytic processes, the number of catalysts tested and evaluated remains limited compared to those used in thermocatalysis.

Tables 2–4 summarize the literature on hydrogen generation from ammonia cracking through photocatalytic, electrocatalytic, and plasma processes, respectively.



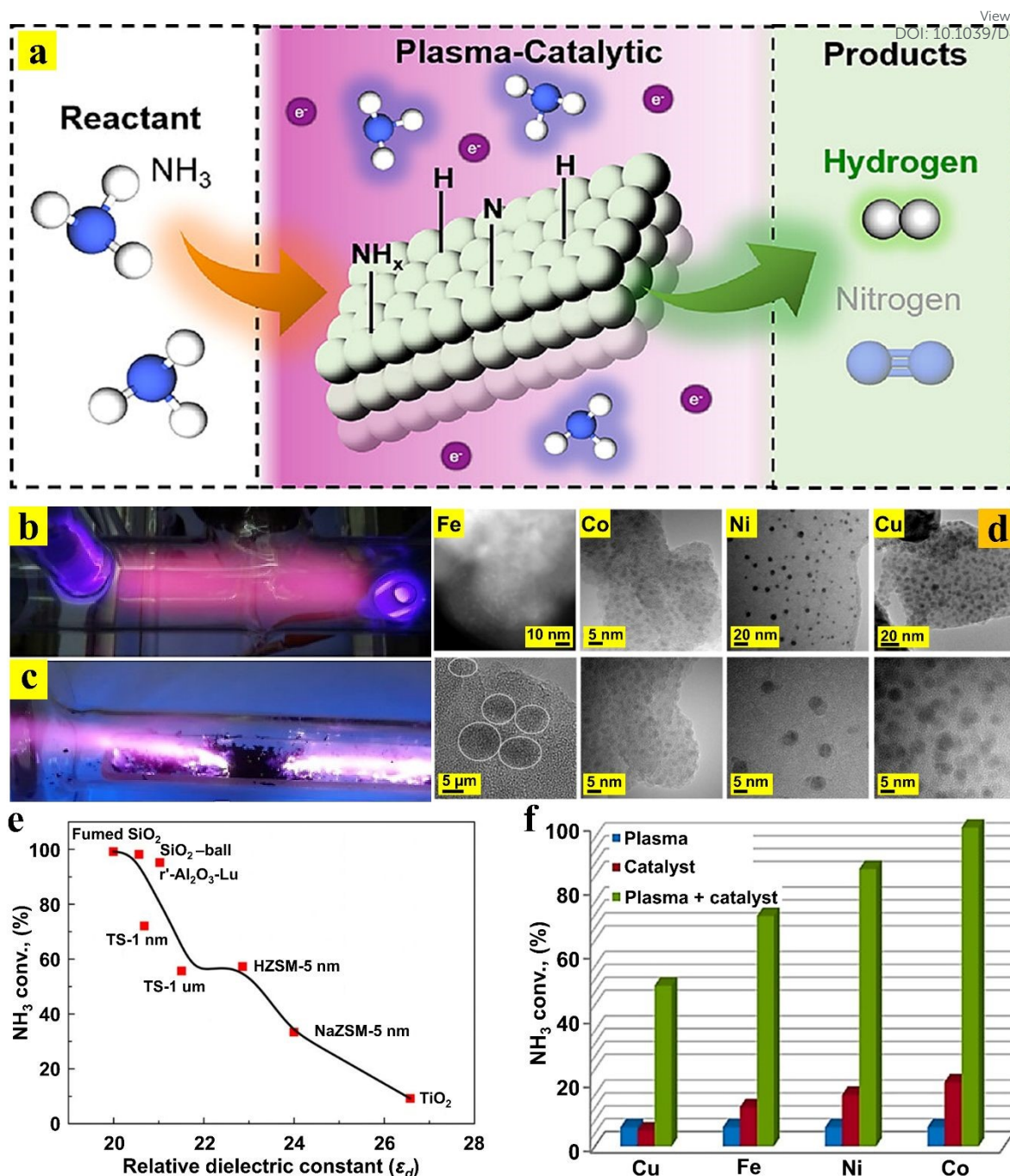


Figure 6. (a) Schematic presentation for the plasma-catalytic NH_3 decomposition. This figure was adapted with the permission of Ref. ⁹². Copyright 2024, American Chemical Society. In situ plasma-assisted catalytic NH_3 conversion system (b) under NTP conditions and (c) glow discharge reactor. These figures were adapted with the permission of Ref. ⁹³. Copyright 2022, MDPI. (d) TEM micrographs of Fe, Co, Ni, and Cu catalysts supported on fumed SiO_2 (reduced in H_2 plasma). (e) NH_3 conversions on Co catalysts on various supports as a function of relative



1 dielectric constants of supports in plasma + catalyst mode (NH_3 feed 40 mL min^{-1} , temperature
2 450°C , supported catalyst 0.88 g , discharge gap 3 mm , discharge frequency 12 kHz). Influence
3 of metals on NH_3 conversion in plasma + catalyst, plasma, and catalyst modes (similar
4 condition for 3b). These figures were adapted with the permission of Ref. ⁹². Copyright 2024,
5 American Chemical Society.

7 **Table 2.** Performance comparison of different catalysts toward photocatalytic NH_3
8 decomposition.

Photocatalyst	Light source	Time	Initial NH_3 concentration	Maximum decomposition ability	Ref.
Pt-TiO ₂ (0.5 wt% Pt)	450 W high pressure Hg lamp	24 h	5 mM	Over 95%	94
Ni/TiO ₂ (0.5 wt% Ni)	500 W Xe lamp	3 h	5 mL, 0.59 mol L^{-1}	131.7 $\mu\text{mol H}_2$ per g- catalyst	19
Ce-doped TiO ₂ (1.4 wt% Ce)	8 W Hg pen-ray lamp	10 h	100 mL, 0.8274 g L^{-1}	1010 mmol H_2 per g- catalyst	95
N-C@TiO ₂	25 W UV lamp	5 min	100 μL aqueous ammonia (30%)	100%	96
MoS ₂ @TiO ₂	25 W UV lamp	7 min	100 μL aqueous ammonia (30%)	91%	97
MoS ₂ /N-doped graphene	300 W UV-visible lamp	8 h	100.0 mg L^{-1}	99.6%	98
Nitrogen-doped rGO/TiO ₂	8 W Hg pen-ray lamp	12 h	0.883 g L^{-1}	$208 \mu\text{mol h}^{-1} \text{ g}^{-1}$	78
GQDs (graphene quantum dots)/CN (g-C ₃ N ₄)	150 W Xe arc lamp	7 h	1.5 mg L^{-1}	90%	99
ZnO/Ag	300 W Xe lamp	2.5 h	1.5 mg L^{-1}	Circa 90%	100

Table 3. Performance comparison of different catalysts toward electrocatalytic NH_3 decomposition.

Catalyst	Catalyst loading (mg cm^{-2})	Electrolyte	Onset potential	Current density (mA cm^{-2})	Scan rate (mV s^{-2})	Ref.
PtIr/C	2.00	1.0 M NH_3	0.470 V_{RHE}	—	10	101
RGO/Pt-Ir	—	1.0 M NH_4OH	— 0.400 $\text{V}_{\text{Ag}/\text{AgCl}}$	20.00 at 0 $\text{V}_{\text{Ag}/\text{AgCl}}$	10	102
Pt ₉₀ Ru ₁₀ /C	1.00	1.0 M NH_4OH + 1.0 M KOH	—	0.920 at — 0.210 $\text{V}_{\text{Hg}/\text{HgO}}$	20	103
Pt _x Ir _{100-x} /MgO	—	0.1 M NH_3 + 0.2 M NaOH	0.530 V_{RHE}	1.00 at 0.710 V_{RHE}	20	104
SnO ₂ -Pt/C	0.028	0.1 M NH_3 + 0.1 M KOH	0.450 V_{RHE}	1.62 at 0.690 V_{RHE}	20	53

3

Table 4. Performance comparison of different catalysts toward plasma-assisted catalytic NH_3 decomposition.

Catalyst	Power	Reactor configuration	Temperature (°C)	Pressure (bar)	Catalyst amount (g)	NH_3 flow rate (L min^{-1})	NH_3 conversion rate (%)	Ref.
FeO	12 kHz 26 W	DBD ^a reactor	410	—	10	0.04	> 99.9	105
Ni-Al ₂ O ₃	23.8 kHz 0–700 W	Non-thermal arc reactor	400–843	—	200	30.00	—	106
Ru-Al ₂ O ₃	10 kHz 12–20 kV	DBD reactor	—	1	—	0.10–1.00	85.7	107
Metal-MgAl ₂ O ₄	1.0–3.5 kHz 10–25 W	DBD reactor	—	1	—	1.00	82.0	108
No catalyst	10 kHz 3.5–22 kV	DBD reactor	—	—	—	0.50	13.0	109

6 Note: ^a dielectric barrier discharge.

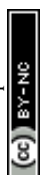
7



5. Other

It is well accepted that the alternative methods for ammonia decomposition, such as electrocatalysis and photocatalysis, often depend on complex catalysts that include costly precious metals. While non-precious metals are more affordable, they tend to exhibit lower catalytic efficiencies and reduced stabilities¹¹⁰. To tackle the challenges in conversion performance, recently, ammonia-water has been recognized as a promising liquid hydrogen carrier with the potential for widespread use in hydrogen generation. However, the hydrogen derived from ammonia-water still poses main challenges. Despite advancements in various methods to enhance the efficiency of hydrogen production from ammonia-water, these techniques have yet to reach a level that is suitable for practical industrial applications¹¹⁰. In this context, Yan *et al.*¹¹⁰ developed a novel, eco-friendly, and ultrafast method for extracting hydrogen from ammonia-water without a catalyst and under ambient conditions using the laser bubbling in liquids (LBL) approach. This technique is entirely different from conventional catalytic methods for hydrogen extraction from ammonia-water. The LBL involves a focused pulsed laser directly beneath the surface of the liquid. When the pulsed laser is applied to ammonia-water, the molecules can be rapidly excited and ionized. This process generates cavitation bubbles at the focus point that achieve transient high temperatures, creating an optimal microspace for efficient hydrogen extraction. It was reported that the real adequate time of laser action on ammonia-water was just 0.36 ms per hour and the actual hydrogen yield reached 93.6 mol h⁻¹ at laser “light-on” time, reflecting the acceptable efficiency of the LBL process.

Another attempt to develop a new approach toward ammonia decomposition was performed by McLennan and Greenwood¹¹¹, discovering that electric discharge in a cathode ray tube can rapidly decompose ammonia. By eliminating the electric current, they focused on the decomposition using only high-speed electron beams, achieving up to 30% decomposition with



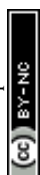
pure ammonia. They also examined the effects of the presence of high-speed electrons (electron spark) on the reaction rate, noting ammonia dilution with N_2 enhanced the reaction while H_2 inhibited it. Similarly, Hirabayashi and Ichihashi¹¹² explored ammonia decomposition using ion beams on various catalysts, identifying vanadium and niobium nitrides ($V_nN_m^+$ and $Nb_nN_m^+$ ($n = 3-6$; $m = n, n-1$)) as promising for hydrogen production.

6. Predicting NH_3 decomposition efficiency by machine learning

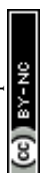
It is well recognized that the broad temperature range of the ammonia decomposition process in practical applications makes it difficult to monitor catalyst changes during the reaction, which is also a major barrier to its practical implementation¹¹³. In addition, discovery of catalysts for NH_3 decomposition is a crucial aspect and has traditionally relied on trial-and-error experiments¹¹³⁻¹¹⁵. Therefore, utilizing DFT and numerical modeling techniques can significantly accelerate research by validating the fundamental mechanisms of ammonia decomposition³⁴.

In recent decades, machine learning (ML) technology has emerged as a powerful tool in designing novel catalysts, understanding composition-structure-property relationships, and analyzing complex data patterns. This efficient computational approach streamlines thermocatalytic ammonia decomposition while minimizing the need for extensive human and material resources in catalyst design¹¹³. The strength of ML algorithms lies in their capacity to learn from historical data without the need for explicit programming. This approach is anticipated to demonstrate high fidelity in identifying optimal operating conditions, not only for NH_3 cracking in the gas phase but also for optimizing CO_2 capture, hydrocracking, and dimethyl ether synthesis¹¹⁶.

To date, several studies have utilized ML models to identify and optimize catalysts for ammonia decomposition. For instance, Williams *et al.*¹¹⁷ assessed the integration of ML with



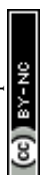
1 high-throughput experimentation to optimize catalyst compositions with low ruthenium
2 content for NH₃ decomposition in a 16-channel parallel reactor system. Their model was
3 developed by training in three progressive stages, utilizing datasets of 3, 22, and 28 catalysts.
4 By analyzing the chemical properties of the secondary metal and reaction temperature, the
5 model effectively predicted ammonia decomposition efficiency. It was found that by
6 employing the random forest algorithm enabled catalyst performance predictions with a mean
7 absolute error of less than 0.16, demonstrating the approach's accuracy and reliability. In
8 another study, Guo *et al.*¹¹³ utilized ML using random forest regression, support vector
9 machines, and gradient boost regression approaches, to statistically analyze ammonia
10 decomposition as a function of catalyst properties and reaction conditions. Their findings
11 revealed a strong positive correlation between catalytic efficiency and reaction temperature,
12 with the gas hourly space velocity (GHSV) emerging as a key factor influencing both ammonia
13 conversion and hydrogen production rates. Notably, optimal decomposition and hydrogen
14 formation were achieved with a total metal loading below 20%wt. It was concluded that among
15 the models tested, the gradient boost regression tree demonstrated strong predictive accuracy,
16 achieving an R^2 greater than 0.85, an RMSE below 13.24, and an MAE under 10.31.
17 Although ML has shown promising results, developed models often tend to be case-specific,
18 limiting their generalizability across different catalyst systems. In addition, traditional ML-
19 guided catalyst screening can be challenging to obtain in new catalytic systems, specifically
20 molecular catalysts for AOR electrocatalysts¹¹⁸. To address these theoretical limitations, recent
21 studies aim to develop an ML model specifically designed to accurately predict the conversion
22 of NH₃ to H₂. By compiling data from published literature, an extensive experimental database
23 was established, and the relationship between independent variables and dependent responses
24 was thoroughly evaluated using statistical analyses and mechanistic insights¹¹³.



Moreover, integrating reaction kinetics into ML framework presents a promising research direction. In this context, understanding the role of reaction kinetics in predicting H₂ formation rates during NH₃ decomposition can provide valuable insights into catalyst behavior and improve predictive accuracy. Additionally, incorporating hydrogen inhibition effects into the ML model will enable researchers to better capture catalyst dynamics, ultimately enhancing performance predictions¹¹³. Notably, the exploration of advanced ML techniques can offer new insights into developing the connections among the characteristics of substances and their catalytic activity, selectivity, and stability of the complex catalytic systems¹¹⁹. In the future, with further research and widespread application of artificial intelligence technologies, ammonia decomposition processes are expected to become more efficient and environmentally sustainable, offering robust support for sustainable development.

7. Further challenges for ammonia decomposition

Extensive research has focused on developing highly active and durable catalysts for ammonia decomposition at minimal temperatures, intending to further lower the temperature to improve efficiency and promote environmentally sustainable processes. It is widely recognized that support for NH₃ decomposition catalysts should exhibit high basicity alongside high conductivity, low concentrations of electron-withdrawing groups, and extensive surface area. Increased basicity can enhance the dispersion of the active metal, thereby facilitating the dehydrogenation of ammonia and the recombinative desorption of surface nitrogen atoms, which are likely the rate-limiting steps of the reaction. Additionally, the electron-donating characteristics of the catalyst can indirectly interact with the support to promote stronger basicity. Consequently, adjusting the basicity of the supports is essential for developing efficient catalysts for NH₃ decomposition. Beyond Ru and Ni catalysts, nitrides, carbides, and perovskites have also gained popularity for optimizing active components in catalytic

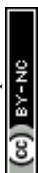


processes. Looking ahead, it will be valuable to explore methods for separating and purifying hydrogen derived from ammonia decomposition in a cost-effective and highly efficient manner. Additionally, microwave and plasma-based decomposition of ammonia merits further investigation.

Moreover, the economic evaluation of a large-scale NH_3 decomposition plant has revealed a significant reliance on the cost of the green ammonia industry. It was demonstrated that lower costs of renewable energy and green ammonia production lead to reduced hydrogen production costs via ammonia decomposition. With a baseline price of green ammonia set at 450 €/ton, the estimated levelized cost of hydrogen (LCOH) was approximately 4.82 € kg^{-1} (in 2019). However, this estimate is influenced by several uncertainties, including the accuracy of total investment cost estimation ($\pm 30\%$), the ammonia decomposition kinetics that affects cracker size and consumption, and the use of ammonia/hydrogen blends as fuel for endothermic reactions in conventional burners. In summary, if green ammonia becomes cost-competitive with fossil-based ammonia, with an estimated price range of 210–215 € ton^{-1} , the cost of producing pressurized hydrogen through ammonia decomposition would be approximately 3.00 €/kg, excluding any potential regulatory or financial incentives¹²⁰.

8. Conclusions and Perspectives

Ammonia, as an ideal hydrogen storage material, is expected to address the challenges of hydrogen storage and transportation in the development of the hydrogen energy industry and overcome the safety problems of hydrogen utilization. Although many ammonia-related studies have contributed to the promotion of ammonia as a favorable alternative renewable resource, further improvements are required in ammonia decomposition to make it a practical H_2 carrier option for on-site generation.



Currently, the great potential of direct ammonia fuel cells for electricity generation in vehicles, hydrogen refilling stations, and ammonia combustion for power requires the decomposition of ammonia under mild conditions. Although progress toward the commercialization of direct ammonia fuel cells is ongoing, in the future, within both distributed and grid power supply systems, a carbon-neutral energy system that combines green ammonia synthesis with ammonia fuel cell technology could become a reality.

In conclusion, combining ML with computational modeling or experiments opens up new possibilities for rapid screening of the catalysts, identifying the performance descriptors, and assisting in catalyst manufacturing. However, further steps are required to couple experimental and theoretical techniques to gain a fundamental understanding, which will inspire researchers to design advanced catalysts for mild-condition ammonia synthesis and decomposition.

Data availability

No primary research results, software or code, have been included and no new data was generated or analyzed as part of this review.

Conflicts of interest

There are no conflicts to declare.

Acknowledgements

The authors acknowledge funding from the US National Science Foundation (NSF) grant (IIP 1939876). The NSF supported this study (Award numbers: 2315268—the Great Lakes Water Innovation Engine and 2314720).



1 **References**

- 2 1. M. El-Shafie, S. Kambara, S. P. Katikaneni, S. N. Paglieri and K. Lee, *International Journal*
3 *of Hydrogen Energy*, 2024, **65**, 126-141.
- 4 2. X. Niu, C. Li, X. Li and Y. Zhang, *Heliyon*, 2024, **10**.
- 5 3. Z. Bao, D. Li, Z. Wang, Y. Wen, L. Jin and H. Hu, *Fuel*, 2024, **373**, 132346.
- 6 4. F. Schüth, R. Palkovits, R. Schlögl and D. S. Su, *Energy & Environmental Science*, 2012, **5**,
7 6278-6289.
- 8 5. J. Li, S. Lai, D. Chen, R. Wu, N. Kobayashi, L. Deng and H. Huang, *Frontiers in Energy*
9 *Research*, 2021, **9**, 760356.
- 10 6. C. Qin, S. Ruan, C. He and L. Zhang, *Colloids and Surfaces A: Physicochemical and*
11 *Engineering Aspects*, 2024, **691**, 133898.
- 12 7. N. Li, C. Zhang, D. Li, W. Jiang and F. Zhou, *Chemical Engineering Journal*, 2024, **495**,
13 153125.
- 14 8. M. Ghasemi, J. Choi, S. M. Ghoreishian, Y. S. Huh and H. Ju, *Journal of The*
15 *Electrochemical Society*, 2023, **170**, 074501.
- 16 9. N. Zhu, Y. Hong, F. Qian and J. Liang, *International Journal of Hydrogen Energy*, 2024, **59**,
17 791-807.
- 18 10. Z. Bao, D. Li, Y. Wu, L. Jin and H. Hu, *International Journal of Hydrogen Energy*, 2024, **53**,
19 848-858.
- 20 11. S. S. Rathore, S. Biswas, D. Fini, A. P. Kulkarni and S. Giddey, *International Journal of*
21 *Hydrogen Energy*, 2021, **46**, 35365-35384.
- 22 12. G. Glenk and S. Reichelstein, *Nature Energy*, 2019, **4**, 216-222.



- 1 13. Y. Gu, Y. Ma, Z. Long, S. Zhao, Y. Wang and W. Zhang, *International Journal of Hydrogen*
2 *Energy*, 2021, **46**, 4045-4054. View Article Online
DOI: 10.1039/D4CC06382A
- 3 14. K. Grubel, H. Jeong, C. W. Yoon and T. Autrey, *Journal of Energy Chemistry*, 2020, **41**, 216-
4 224.
- 5 15. I. Cabria, *International Journal of Hydrogen Energy*, 2024, **50**, 160-177.
- 6 16. Z. Yan, H. Liu, Z. Hao, M. Yu, X. Chen and J. Chen, *Chemical Science*, 2020, **11**, 10614-
7 10625.
- 8 17. C. Chen, K. Wu, H. Ren, C. Zhou, Y. Luo, L. Lin, C. Au and L. Jiang, *Energy & Fuels*, 2021,
9 **35**, 11693-11706.
- 10 18. P. Adamou, S. Bellomi, S. Hafeez, E. Harkou, S. M. Al-Salem, A. Villa, N. Dimitratos, G.
11 Manos and A. Constantinou, *Catalysis Today*, 2023, **423**, 114022.
- 12 19. A. Utsunomiya, A. Okemoto, Y. Nishino, K. Kitagawa, H. Kobayashi, K. Taniya, Y.
13 Ichihashi and S. Nishiyama, *Applied Catalysis B: Environmental*, 2017, **206**, 378-383.
- 14 20. S. Mukherjee, S. V. Devaguptapu, A. Sviripa, C. R. F. Lund and G. Wu, *Applied Catalysis B:*
15 *Environmental*, 2018, **226**, 162-181.
- 16 21. S. Sun, Q. Jiang, D. Zhao, T. Cao, H. Sha, C. Zhang, H. Song and Z. Da, *Renewable and*
17 *Sustainable Energy Reviews*, 2022, **169**, 112918.
- 18 22. S. F. Yin, B. Q. Xu, X. P. Zhou and C. T. Au, *Applied Catalysis A: General*, 2004, **277**, 1-9.
- 19 23. S. M. Ghoreishian, K. Shariati, Y. S. Huh and J. Lauterbach, *Chemical Engineering Journal*,
20 2023, **467**, 143533.
- 21 24. T. E. Bell and L. Torrente-Murciano, *Topics in Catalysis*, 2016, **59**, 1438-1457.



- 1 25. Y. Sun, W. Zeng, Y. Yang, Q. Wu and C. Zou, *Chemical Engineering Journal*, 2024, **502**,
 2 158043. View Article Online
DOI: 10.1039/D4CC06382A
- 3 26. N. Morlanés, S. P. Katikaneni, S. N. Paglieri, A. Harale, B. Solami, S. M. Sarathy and J.
 4 Gascon, *Chemical Engineering Journal*, 2021, **408**, 127310.
- 5 27. N. Zecher-Freeman, H. Zong, P. Xie and C. Wang, *Current Opinion in Green and*
 6 *Sustainable Chemistry*, 2023, **44**, 100860.
- 7 28. Z.-W. Wu, X. Li, Y.-H. Qin, L. Deng, C.-W. Wang and X. Jiang, *International Journal of*
 8 *Hydrogen Energy*, 2020, **45**, 15263-15269.
- 9 29. K. G. Kirste, K. McAulay, T. E. Bell, D. Stoian, S. Laassiri, A. Daisley, J. S. J. Hargreaves,
 10 K. Mathisen and L. Torrente-Murciano, *Applied Catalysis B: Environmental*, 2021, **280**,
 11 119405.
- 12 30. N. Morlanés, S. Sayas, G. Shterk, S. P. Katikaneni, A. Harale, B. Solami and J. Gascon,
 13 *Catalysis Science Technology*, 2021, **11**, 3014-3024.
- 14 31. E. Fu, Y. Qiu, H. Lu, S. Wang, L. Liu, H. Feng, Y. Yang, Z. Wu, Y. Xie, F. Gong and R.
 15 Xiao, *Fuel Processing Technology*, 2021, **221**, 106945.
- 16 32. I. Lucentini, A. Casanovas and J. Llorca, *International Journal of Hydrogen Energy*, 2019,
 17 **44**, 12693-12707.
- 18 33. V. D. B. C. Dasireddy, Š. Hajduk, F. Ruiz-Zepeda, J. Kovač, B. Likozar and Z. C. Orel, *Fuel*
 19 *Processing Technology*, 2021, **215**, 106752.
- 20 34. T. Han, L. Wei, S. Xie, Y. Liu, H. Dai and J. Deng, *Industrial Chemistry & Materials*, 2025.
- 21 35. Z. Zhao, Z. Liu, M. Li, Y. Yang, L. Deng, Y. Zhao, B. Dou and F. Bin, *Separation and*
 22 *Purification Technology*, 2025, **360**, 131144.



- 1 36. D. Liang, C. Feng, L. Xu, D. Wang, Y. Liu, X. Li and Z. Wang, *Catalysis Science & Technology*, 2023, **13**, 3614-3628. View Article Online
DOI: 10.1039/D4CC06382A
- 2
- 3 37. J. C. Verschoor, P. E. de Jongh and P. Ngene, *Current Opinion in Green and Sustainable*
- 4 *Chemistry*, 2024, **50**, 100965.
- 5 38. Y. Qiu, E. Fu, F. Gong and R. Xiao, *International Journal of Hydrogen Energy*, 2022, **47**,
- 6 5044-5052.
- 7 39. G. Li, H. Zhang, X. Yu, Z. Lei, F. Yin and X. He, *International Journal of Hydrogen Energy*,
- 8 2022, **47**, 12882-12892.
- 9 40. H. Tang, Y. Wang, W. Zhang, Z. Liu, L. Li, W. Han and Y. Li, *Journal of Solid State*
- 10 *Chemistry*, 2021, **295**, 121946.
- 11 41. G. Li, X. Yu, F. Yin, Z. Lei, H. Zhang and X. He, *Catalysis Today*, 2022, **402**, 45-51.
- 12 42. M. Pinzón, O. Avilés-García, A. R. de la Osa, A. de Lucas-Consuegra, P. Sánchez and A.
- 13 Romero, *Sustainable Chemistry and Pharmacy*, 2022, **25**, 100615.
- 14 43. A. Jedynak, Z. Kowalczyk, D. Szmigiel, W. Raróg and J. Zieliński, *Applied Catalysis A:*
- 15 *General*, 2002, **237**, 223-226.
- 16 44. J. C. Ganley, F. Thomas, E. Seebauer and R. I. J. C. L. Masel, 2004, **96**, 117-122.
- 17 45. H. Li, L. Guo, J. Qu, X. Fang, Y. Fu, J. Duan, W. Wang and C. Li, *International Journal of*
- 18 *Hydrogen Energy*, 2023, **48**, 8985-8996.
- 19 46. J. Zhang, M. Comotti, F. Schüth, R. Schlögl and D. S. Su, *Chemical Communications*, 2007,
- 20 1916-1918.
- 21 47. L. Li, F. Chen, J. Shao, Y. Dai, J. Ding and Z. Tang, *International Journal of Hydrogen*
- 22 *Energy*, 2016, **41**, 21157-21165.



- 1 48. M. Feyen, C. Weidenthaler, R. Güttel, K. Schlichte, U. Holle, A.-H. Lu and F. Schüth, *Chemistry – A European Journal*, 2011, **17**, 598-605.
- 2
- 3 49. H. Zhang, Y. A. Alhamed, A. Al-Zahrani, M. Daous, H. Inokawa, Y. Kojima and L. A. Petrov, *International Journal of Hydrogen Energy*, 2014, **39**, 17573-17582.
- 4
- 5 50. T. A. Le, Y. Kim, H. W. Kim, S.-U. Lee, J.-R. Kim, T.-W. Kim, Y.-J. Lee and H.-J. Chae, *Applied Catalysis B: Environmental*, 2021, **285**, 119831.
- 6
- 7 51. S. Podila, Y. A. Alhamed, A. A. AlZahrani and L. A. Petrov, *International Journal of Hydrogen Energy*, 2015, **40**, 15411-15422.
- 8
- 9 52. M. Pinzón, A. Romero, A. de Lucas-Consuegra, A. R. de la Osa and P. Sánchez, *Catalysis Today*, 2022, **390-391**, 34-47.
- 10
- 11 53. K. Okura, T. Okanishi, H. Muroyama, T. Matsui and K. Eguchi, *Applied Catalysis A: General*, 2015, **505**, 77-85.
- 12
- 13 54. N. Zhu, F. Yang, Y. Hong and J. Liang, *International Journal of Hydrogen Energy*, 2025, **98**, 1243-1261.
- 14
- 15 55. I. Lucentini, X. Garcia, X. Vendrell, J. J. I. Llorca and E. C. Research, 2021, **60**, 18560-18611.
- 16
- 17 56. X. Huang, K. Lei, Y. Mi, W. Fang and X. Li, *Molecules*, 2023, **28**, 5245.
- 18
- 19 57. S. Mirsadeghi, S. M. Ghoreishian, H. Zandavar, R. Behjatmanesh-Ardakani, E. Naghian, M. Ghoreishian, A. Mehrani, N. Abdolhoseinpoor, M. R. Ganjali, Y. S. Huh and S. M. Pourmortazavi, *Journal of Environmental Chemical Engineering*, 2023, **11**, 109106.
- 20
- 21 58. S. M. Ghoreishian, K. S. Ranjith, B. Park, S.-K. Hwang, R. Hosseini, R. Behjatmanesh-Ardakani, S. M. Pourmortazavi, H. U. Lee, B. Son, S. Mirsadeghi, Y.-K. Han and Y. S. Huh, *Chemical Engineering Journal*, 2021, **419**, 129530.
- 22
- 23



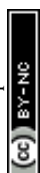
- 1 59. S. M. Ghoreishian, K. S. Ranjith, M. Ghasemi, B. Park, S.-K. Hwang, N. Irannejad, M. Norouzi, S. Y. Park, R. Behjatmanesh-Ardakani, S. M. Pourmortazavi, S. Mirsadeghi, Y.-K. Han and Y. S. Huh, *Chemical Engineering Journal*, 2023, **452**, 139435. View Article Online
DOI: 10.1039/D4CC06382A
- 2
- 3
- 4 60. H. Martin, C. Ruck, M. Schmidt, S. Sell, S. Beutner, B. Mayer and R. Walsh, *Pure and Applied Chemistry*, 1999, **71**, 2253-2262.
- 5
- 6 61. B. G. Petri, R. J. Watts, A. L. Teel, S. G. Huling and R. A. Brown, in *In situ chemical oxidation for groundwater remediation*, 2011, pp. 33-88.
- 7
- 8 62. Z. Yong and T. Ma, *Angewandte Chemie International Edition*, 2023, **62**, 202308980.
- 9 63. M. Reli, M. Edelmannová, M. Šihor, P. Praus, L. Svoboda, K. K. Mamulová, H. Otoupalíková, L. Čapek, A. Hospodková, L. Obalová and K. Kočí, *International Journal of Hydrogen Energy*, 2015, **40**, 8530-8538.
- 10
- 11
- 12 64. H. Kominami, H. Nishimune, Y. Ohta, Y. Arakawa and T. Inaba, *Applied Catalysis B: Environmental*, 2012, **111-112**, 297-302.
- 13
- 14 65. C. Jo, S. Surendran, M.-C. Kim, T.-Y. An, Y. Lim, H. Choi, G. Janani, S. Cyril Jesudass, D. Jun Moon, J. Kim, J. Young Kim, C. Hyuck Choi, M. Kim, J. Kyu Kim and U. Sim, *Chemical Engineering Journal*, 2023, **463**, 142314.
- 15
- 16
- 17 66. H. Shi, C. Li, L. Wang, W. Wang, J. Bian and X. Meng, *Journal of Alloys and Compounds*, 2023, **933**, 167815.
- 18
- 19 67. D. Yuan, F. Xie, K. Li, Q. Guan, J. Hou, S. Yang, G. Han, X. San, J. Hao and Y. Li, *Applied Surface Science*, 2023, **613**, 155973.
- 20
- 21 68. S. Zhang, Z. He, X. Li, J. Zhang, Q. Zang and S. Wang, *Nanoscale Advances*, 2020, **2**, 3610-3623.
- 22



- 1 69. J. Lin, Y. Wang, W. Tian, H. Zhang, H. Sun and S. Wang, *ACS Catalysis*, 2023, **13**, 11711-11722. New Article Online
DOI: 10.1039/D4CC06382A
- 2 11722.
- 3 70. J. Dzíbelová, S. M. H. Hejazi, V. Šedajová, D. Panáček, P. Jakubec, Z. Baďura, O. Malina, J. Kašlík, J. Filip, Š. Kment, M. Otyepka and R. Zbořil, *Applied Materials Today*, 2023, **34**, 101881.
- 4 71. S. Zhang, L. Yan, H. Jiang, L. Yang, Y. Zhao, X. Yang, Y. Wang, J. Shen and X. Zhao, *ACS Applied Materials & Interfaces*, 2022, **14**, 9036-9045.
- 5 72. Z. Wang, S. D. Young, B. R. Goldsmith and N. Singh, *Journal of Catalysis*, 2021, **395**, 143-154.
- 6 73. Y. Tian, Z. Mao, L. Wang and J. Liang, *Small Structures*, 2023, **4**, 2200266.
- 7 74. R. Sen, S. Das, A. Nath, P. Maharana, P. Kar, F. Verpoort, P. Liang and S. Roy, *Frontiers in Chemistry*, 2022, **10**, 861604.
- 8 75. A. AlZaabi, F. AlMarzooqi and D. Choi, *International Journal of Hydrogen Energy*, 2024, **94**, 23-52.
- 9 76. K. Goshome, T. Yamada, H. Miyaoka, T. Ichikawa and Y. Kojima, *International Journal of Hydrogen Energy*, 2016, **41**, 14529-14534.
- 10 77. N. Hanada, S. Hino, T. Ichikawa, H. Suzuki, K. Takai and Y. Kojima, *Chemical communications*, 2010, **46**, 7775-7777.
- 11 78. Z. Wu, N. Ambrožová, E. Eftekhari, N. Aravindakshan, W. Wang, Q. Wang, S. Zhang, K. Kočí and Q. Li, *Emergent Materials*, 2019, **2**, 303-311.
- 12 79. N. M. Adli, H. Zhang, S. Mukherjee and G. Wu, *Journal of The Electrochemical Society*, 2018, **165**, J3130.
- 13
- 14
- 15
- 16
- 17
- 18
- 19
- 20
- 21
- 22



- 1 80. J.-J. Zhong, S.-P. Huang, J.-F. Gu, Y. Li, K.-N. Ding, Y.-F. Zhang, W. Lin and W.-K. Chen, *Applied Surface Science*, 2023, **609**, 155280. View Article Online
DOI: 10.1039/D4CC06382A
- 2
- 3 81. J. A. Herron, P. Ferrin and M. Mavrikakis, *The Journal of Physical Chemistry C*, 2015, **119**,
- 4 14692-14701.
- 5 82. P. Modisha and D. Bessarabov, *International Journal of Electrochemical Science*, 2016, **11**,
- 6 6627-6635.
- 7 83. B.-X. Dong, H. Tian, Y.-C. Wu, F.-Y. Bu, W.-L. Liu, Y.-L. Teng and G.-W. Diao,
- 8 *International Journal of Hydrogen Energy*, 2016, **41**, 14507-14518.
- 9 84. M. Idamakanti, E. B. Ledesma, R. R. Ratnakar, M. P. Harold, V. Balakotaiah and P. Bollini,
- 10 *ACS Engineering Au*, 2023, **4**, 71-90.
- 11 85. Y.-S. Son, K.-H. Kim, K.-J. Kim and J.-C. Kim, *Plasma Chemistry and Plasma Processing*,
- 12 2013, **33**, 617-629.
- 13 86. D. Varisli, C. Korkusuz and T. Dogu, *Applied Catalysis B: Environmental*, 2017, **201**, 370-
- 14 380.
- 15 87. M. Akiyama, K. Aihara, T. Sawaguchi, M. Matsukata and M. Iwamoto, *International Journal*
- 16 *of Hydrogen Energy*, 2018, **43**, 14493-14497.
- 17 88. P. Peng, J. Su and H. Breunig, *Energy Conversion and Management*, 2023, **288**, 117166.
- 18 89. Z. Wang, H. Zhang, Z. Ye, G. He, C. Liao, J. Deng, G. Lei, G. Zheng, K. Zhang, F. Gou and
- 19 X. Mao, *International Journal of Hydrogen Energy*, 2024, **49**, 1375-1385.
- 20 90. K. H. R. Rouwenhorst, Y. Engelmann, K. van 't Veer, R. S. Postma, A. Bogaerts and L.
- 21 Lefferts, *Green Chemistry*, 2020, **22**, 6258-6287.



- 1 91. L. Wang, Y. Yi, Y. Zhao, R. Zhang, J. Zhang and H. Guo, *ACS Catalysis*, 2015, **5**, 4167-4174. View Article Online
DOI: 10.1039/D4CC06382A
- 2 4174.
- 3 92. N. Wang, H. O. Otor, G. Rivera-Castro and J. C. Hicks, *ACS Catalysis*, 2024, **14**, 6749-6798.
- 4 93. J. Moszczyńska, X. Liu and M. Wiśniewski, *International Journal of Molecular Sciences*,
5 2022, **23**, 9638.
- 6 94. S. Shibuya, Y. Sekine and I. Mikami, *Applied Catalysis A: General*, 2015, **496**, 73-78.
- 7 95. M. Reli, N. Ambrožová, M. Šihor, L. Matějová, L. Čapek, L. Obalová, Z. Matěj, A. Kotarba
8 and K. Kočí, *Applied Catalysis B: Environmental*, 2015, **178**, 108-116.
- 9 96. Y.-N. Li, Z.-Y. Chen, S.-J. Bao, M.-Q. Wang, C.-L. Song, S. Pu and D. Long, *Chemical
10 Engineering Journal*, 2018, **331**, 383-388.
- 11 97. S. Pu, D. Long, M.-Q. Wang, S.-J. Bao, Z. Liu, F. Yang, H. Wang and Y. Zeng, *Materials
12 Letters*, 2017, **209**, 56-59.
- 13 98. H. Zhang, Q.-Q. Gu, Y.-W. Zhou, S.-Q. Liu, W.-X. Liu, L. Luo and Z.-D. Meng, *Applied
14 Surface Science*, 2020, **504**, 144065.
- 15 99. R. Wang, T. Xie, Z. Sun, T. Pu, W. Li and J.-P. Ao, *RSC advances*, 2017, **7**, 51687-51694.
- 16 100. W. Guo and H. Liu, *Chemical Research in Chinese Universities*, 2017, **33**, 129-134.
- 17 101. B. Achrai, Y. Zhao, T. Wang, G. Tamir, R. Abbasi, B. P. Setzler, M. Page, Y. Yan and S.
18 Gottesfeld, *Journal of The Electrochemical Society*, 2020, **167**, 134518.
- 19 102. L. Cunci, C. V. Rao, C. Velez, Y. Ishikawa and C. R. Cabrera, *Electrocatalysis*, 2013, **4**, 61-
20 69.
- 21 103. J. C. M. Silva, S. Ntais, É. Teixeira-Neto, E. V. Spinacé, X. Cui, A. O. Neto and E. A.
22 Baranova, *International Journal of Hydrogen Energy*, 2017, **42**, 193-201.



- 1 104. N. Sacré, M. Duca, S. Garbarino, R. Imbeault, A. Wang, A. Hadj Youssef, J. Galipaud, C. View Article Online
2 Hufnagel, A. Ruediger and L. Roue, *ACS Catalysis*, 2018, **8**, 2508-2518. DOI: 10.1039/D4CC06382A
- 3 105. L. Wang, Y. Zhao, C. Liu, W. Gong and H. Guo, *Chemical communications*, 2013, **49**, 3787-
4 3789.
- 5 106. Q. F. Lin, Y. M. Jiang, C. Z. Liu, L. W. Chen, W. J. Zhang, J. Ding and J. G. Li, *Energy*
6 *Reports*, 2021, **7**, 4064-4070.
- 7 107. M. El-Shafie, S. Kambara and Y. Hayakawa, *Journal of the Energy Institute*, 2021, **99**, 145-
8 153.
- 9 108. J. A. Andersen, K. van 't Veer, J. M. Christensen, M. Østberg, A. Bogaerts and A. D. Jensen,
10 *Chemical Engineering Science*, 2023, **271**, 118550.
- 11 109. Y. Hayakawa, S. Kambara and T. Miura, *International Journal of Hydrogen Energy*, 2020,
12 **45**, 32082-32088.
- 13 110. B. Yan, Y. Li, W. Cao, Z. Zeng, P. Liu, Z. Ke and G. Yang, *Journal of the American*
14 *Chemical Society*, 2024, **146**, 4864-4871.
- 15 111. J. C. McLennan and G. Greenwood, *Proceedings of the Royal Society of London*, 1928, **120**,
16 283-295.
- 17 112. S. Hirabayashi and M. Ichihashi, *International Journal of Mass Spectrometry*, 2016, **407**, 86-
18 91.
- 19 113. W. Guo, A. Shafizadeh, H. Shahbeik, S. Rafiee, S. Motamedi, S. A. Ghafarian Nia, M. H.
20 Nadian, F. Li, J. Pan, M. Tabatabaei and M. Aghbashlo, *Journal of Energy Storage*, 2024, **89**,
21 111688.
- 22 114. E. Soltanmohammadi and N. Hikmet, *Journal of Data Analysis Information Processing*,
23 2024, **12**, 544-565.



- 1 115. E. Soltanmohammadi, A. Dilek and N. Hikmet, *Journal of Data Analysis Information Processing*, 2024, **13**, 46-65. View Article Online
DOI: 10.1039/D4CC06382A
- 2
- 3 116. D.-N. Vo, J. Hun Chang, S.-H. Hong and C.-H. Lee, *Chemical Engineering Journal*, 2023,
- 4 **475**, 146195.
- 5 117. T. Williams, K. McCullough and J. A. Lauterbach, *Chemistry of Materials*, 2019, **32**, 157-
- 6 165.
- 7 118. Z.-H. Lyu, J. Fu, T. Tang, J. Zhang and J.-S. Hu, *EnergyChem*, 2023, **5**, 100093.
- 8 119. H. Mashhadimoslem, M. Safarzadeh Khosrowshahi, M. Delpisheh, C. Convery, M.
- 9 Rezakazemi, T. M. Aminabhavi, M. Kamkar and A. Elkamel, *Chemical Engineering Journal*,
- 10 2023, **474**, 145661.
- 11 120. C. Makhoulfi and N. Kezibri, *International Journal of Hydrogen Energy*, 2021, **46**, 34777-
- 12 34787.
- 13



No primary research results, software or code have been included and no new data were generated or analysed as part of this review.

